High contrast reflection modulation near 1.55μm in InP 2D photonic crystals on silicon wafer

G. Vecchi, F. Raineri, I. Sagnes, K-H. Lee, S. Guilet, L. Le Gratiet, A. Talneau, A. Levenson and R. Raj

Laboratoire de Photonique et de Nanostructures (CNRS UPR20), Route de Nozay, 91460 Marcoussis, France
gabriele.vecchi@lpn.cnrs.fr

F. Van Laere, G. Roelkens, D. Van Thourhout and R. Baets

Ghent University – IMEC, Department of Information Technology, Sint-Pietersnieuwstraat 41, 9000 Ghent, Belgium

Abstract: We report on reflection modulation results near 1.55 µm in InP-based two-dimensional photonic crystals. The fabrication technology uses a polymeric bonding technique to integrate the InP thin-slab onto a Silicon wafer. Reflectivity modulation greater than 90% is obtained by pumping at 810 nm with optical excitation densities of 15 µJ/cm^2. The resulting optical broadband modulation is based on the saturation of absorption of InGaAs quantum wells at a photonic mode frequency tunable by lithography.

©2006 Optical Society of America

OCIS codes: (130.5990) Semiconductors; (130.3130) Integrated optics materials; (190.4720) Optical nonlinearities of condensed matter; (230.4110) Modulators.

References and links

1. G.T. Reed and A.P. Knights, *Silicon Photonics: An Introduction* (Wiley, 2004).
2. A. Liu, R. Jones, L. Liao, D. Samara-Rubio, D. Rubin, O. Cohen, R. Nicolaescu, and M. Paniccia, "A high-speed silicon optical modulator based on a metal-oxide-semiconductor capacitor," Nature **427**, 615-618 (2004).
3. S.F. Preble, Q. Xu, B. S. Schmidt and M. Lipson, "Ultrafast all-optical modulation on a silicon chip," Opt. Lett. **30**, 2891-2893 (2005).
4. F. C. Ndi, J. Toulouse, T. Hodson and D. W. Prather, "Optically tunable silicon photonic crystal microcavities," Opt. Express **14,** 4835-4840 (2006).
5. S. W. Leonard, H. M. van Driel, J. Schilling and R. B. Wehrspohn, "Ultrafast band-edge tuning of a two-dimensional silicon photonic crystal via free-carrier injection," Phys. Rev. B **66**, 161102 (R) (2002).
6. F. Raineri, C. Cojocaru, P. Monnier, A. Levenson, R. Raj, C. Seassal, X. Letartre, and P. Viktorovitch, "Ultrafast dynamics of the third-order nonlinear response in a two-dimensional InP-based photonic crystal," Appl. Phys. Lett. **85**, 1880-1882 (2004).
7. H. Nakamura, Y. Sugimoto, K. Kanamoto, N. Ikeda, Y. Tanaka, Y. Nakamura, S. Ohkouchi, Y. Watanabe, K. Inoue, H. Ishikawa and K. Asakawa, "Ultra-fast photonic crystal/quantum dot all-optical switch for future photonic networks," Opt. Express **12,** 6606-6614 (2004).
8. A. M. Yacomotti, F. Raineri, G. Vecchi, I. Sagnes, M. Strassner, L. Le Gratiet, R. Raj and A. Levenson, "Ultra-fast nonlinear response around 1.5 µm in 2D AlGaAs/AlOx photonic crystal," Appl. Phys. B **81**, 333-336 (2005).
9. A. D. Bristow, D. O. Kundys, A. Z. García-Deníz, J.-P. R. Wells, A. M. Fox, M. S. Skolnick, D. M. Whittaker, A. Tahraoui, T. F. Krauss and J. S. Roberts, "Enhanced all-optical tuning of leaky eigenmodes in photonic crystal waveguides," Opt. Lett. **31**, 2284-2286 (2006).
10. F. Raineri, G. Vecchi, C. Cojocaru, A. M. Yacomotti, C. Seassal, X. Letartre, P. Viktorovitch, R. Raj, and A. Levenson, "Optical amplification in two-dimensional photonic crystals," Appl. Phys. Lett. **86**, 091111 (2005).
11. M. Notomi, A. Shinya, S. Mitsugi, G. Kira, E. Kuramochi and T. Tanabe, "Optical bistable switching action of Si high-Q photonic-crystal nanocavities," Opt. Express **13,** 2678-2687 (2005).
12. A. M. Yacomotti, F. Raineri, G. Vecchi, P. Monnier, R. Raj, A. Levenson, B. Ben Bakir, C. Seassal, X. Letartre, P. Viktorovitch L. Di Cioccio and J. M. Fedeli, "All-optical bistable band-edge Bloch modes in a two-dimensional photonic crystal," Appl. Phys. Lett. **88**, 231107 (2006).
13. O. Painter, R. K. Lee, A. Scherer, A. Yariv, J. D. O'Brien, P. D. Dapkus and I. Kim, "Two-dimensional photonic band-gap defect mode laser," Science **284**, 1819–1821 (1999).

14. H. T. Hattori, C. Seassal, X. Letartre, P. Rojo-Romeo, J. L. Leclercq, P. Viktorovitch M. Zussy, L. di Cioccio, L. El Melhaoui and J.-M. Fedeli, "Coupling analysis of heterogeneous integrated InP based photonic crystal triangular lattice band-edge lasers and silicon waveguides," Opt. Express **13,** 3310-3322 (2005).
15. T. Maruyama, T. Okumura, S. Sakamoto, K. Miura, Y. Nishimoto and S. Arai, "GaInAsP/InP membrane BH-DFB lasers directly bonded on SOI substrate," Opt. Express **14,** 8184-8188 (2006).
16. C. Symonds, J. Dion, I. Sagnes, M. Dainese, M. Strassner, L. Leroy and J.-L. Oudar, "High performance 1.55 µm vertical external cavity surface emitting laser with broadband integrated dielectric-metal mirror," Electron. Lett. **40,** 734-735 (2004).
17. G. Roelkens, D. Van Thourhout, R. Baets R. Nötzel, and M. Smit, "Laser emission and photodetection in an InP/InGaAsP layer integrated on and coupled to a Silicon-on-Insulator waveguide circuit," Opt. Express **14,** 8154-8159 (2006).
18. P. N. Butcher and D. Cotter, *The elements of nonlinear optics* (Cambridge University Press, 1990).
19. K. Wakita, *Semiconductor Optical Modulators* (Kluwer Academic Publishers, 1998).
20. T. L. Worchesky, K. J. Ritter, R. Martin and B. Lane, "Large arrays of spatial light modulators hybridized to silicon integrated circuits," Appl. Opt. **35**, 1180-1186 (1996).
21. F. Raineri, G. Vecchi, A. M. Yacomotti, C. Seassal, P. Viktorovitch, R. Raj and A. Levenson, "Doubly resonant photonic crystal for efficient laser operation: Pumping and lasing at low group velocity photonic modes", Appl. Phys. Lett. **86**, 011116 (2005).
22. L.V. Dao, M. Gal, C. Carmody, H. H. Tan and C. Jagadish, "A comparison of impurity-free and ion-implantation-induced intermixing of InGaAs/InP quantum wells," J. Appl. Phys. **88**, 5252-5254 (2000).

1. Introduction

A lot of research activity is currently addressed towards obtaining optical functionalities on top of a silicon chip [1-4]. One possibility is to use an all silicon-based optical circuit where the inherent properties of this material are exploited to manipulate light. An alternative approach relies on the fabrication of hybrid structures which integrate active III-V materials-based optical devices to passive Silicon-based waveguides.

In this context, III-V based two dimensional photonic crystals (2D PhCs) hold a lot of promise as shown by the recent demonstration of several optical functions such as ultrafast switching [5-9], gain [10], bistability [11,12], and laser emission [13]. Indeed, these periodic structures, with their lattice constants of the order of the light wavelength, enable strong light matter-interaction leading to low power need for obtaining the desired nonlinear regimes.

Several technologies have been proposed to bond III-V semiconductors on Silicon, like SiO_2-SiO_2 molecular wafer bonding [14], direct bonding [15] or Au/In dry bonding [16]. We consider here for the heterogeneous integration of the 2D PhC on a silicon wafer, the use of benzocyclobutene (BCB) for bonding. This technique has recently been used to integrate InP-InGaAsP edge emitting lasers on Silicon on insulator waveguides [17]. Among the advantages of this method, we point out its relative simplicity with a potential towards low-cost mass production, the optical transparency of BCB at telecom wavelengths and the high refractive index contrast with semiconductors.

In this paper, we report on the integration, for the first time, of III-V based 2D PhC on a silicon substrate using BCB. The heterogeneous structure is fabricated with the view to obtaining a fast optical modulator. Its operation is based on the change of the PhC response at the frequency of a band edge mode, induced by the saturation of the absorption of the quantum wells embedded in the slab. We demonstrate 90% contrast modulation of reflectivity at 1.53 µm by pumping at 810 nm.

2. Design and fabrication of the 2D PhC modulator on Silicon

Our work is based on the exploitation of the dynamical nonlinearities of quantum-wells (QWs) to achieve the modulation of the 2D PhC optical response. These nonlinearities are induced by creation of carriers, making possible a control over absorption and refractive index of the material [18]. QW optical modulators have been extensively studied in the past. Several configurations for device operation have been proposed, often cavity-assisted in order to simultaneously improve performance and reduce power need [19]. 2D PhCs containing QWs have already been considered for modulation purpose [6, 8-9]. The proposed solutions consisted in using the nonlinear refractive index change to shift the wavelength of a photonic

crystal resonance, thus modifying the reflectivity. In these papers, the PhC is designed so that the photonic resonances occur in a spectral region of very weak absorption, using thereby dispersive nonlinear effects. For example, in Ref. [6], the photonic mode is placed very far in the Urbach tail of the absorption of the quantum wells. The performance, in terms of bandwidth and pump power requirements, is dependent on the spectral width of the resonance, i.e. the quality factor Q. Of course, as Q increases, the pump power necessary to fully shift the resonance lowers, however, the bandwidth narrows.

In this work, the 2D PhC is designed so that a slow Bloch mode is spectrally placed at the maximum of the QWs absorption. In this case, as carriers are injected, QWs absorption saturates, reducing the intrinsic losses of the Bloch mode resonator, giving a change of reflectivity at the resonance wavelength. The amount of pump power required to bleach the QWs absorption does not depend on the quality factor of the photonic resonance, which, therefore, can be tailored to fit the bandwidth requirement. Also, this slow Bloch mode is placed at the Γ point of the Brillouin zone (normal incidence with respect to plane of periodicity) in order to enable surface operation. "Surface-normal" modulators are particularly attractive for parallel optical data processing [20] as the QW modulator devices may be assembled in 2D arrays.

The 2D PhC under investigation is a graphite lattice of air holes drilled in a 265 nm InP slab incorporating four lattice-matched $In_{0.53}Ga_{0.47}As$ QWs emitting around 1.53 µm, as indicated in Fig. 1(a). The InP membrane was grown by MOCVD and then transferred onto a silicon substrate through BCB bonding [17]. The air holes are patterned into the transferred InP slab using inductive plasma etching through a silicon nitride mask obtained by e-beam lithography and reactive ion etching. Note that the slab thickness is chosen to be $\lambda/2\tilde{n}$, where $\lambda = 1.55$ µm and ñ is the mean index of refraction of the patterned slab, ensuring good vertical optical confinement. The vertical hetero-structure and a scanning electron micrograph of the sample are shown in Figs. 1(b) and 1(c), respectively.
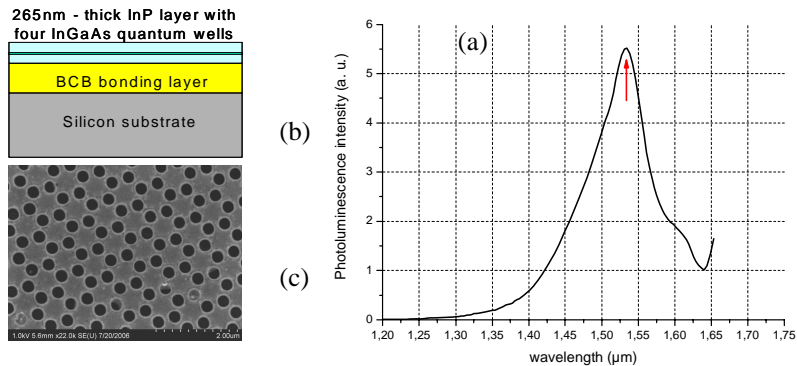

Fig. 1. (a). photoluminescence spectrum of InGaAs QWs (b) layout of the hetero-structure (c) Scanning electron micrograph of the graphite PhC.

Several 50 µm x 50 µm 2D PhCs were drilled in the InP slab, each one defined using a different e-beam dose exposure, in order to obtain a range of tunable frequencies of the photonic bands. As has been described in Ref. [21], several modes occur at the Γ point of the Brillouin zone for such graphite lattices. Here we choose the lattice parameters so that a low-Q photonic mode, giving a broad bandwidth, is placed at ~1.53 µm, near the maximum of QWs absorption [see arrow on Fig. 1(a)]. The graphite lattice constant is 1.3 µm and the hole diameter varies from 190 to 260 nm. Every 50 µm x 50 µm patterned area is composed of four 25 µm x 25 µm adjacent areas (in the following labeled A, B, C, and D), characterized by a specific value for the air-hole diameter. As a result, each 50 µm x 50 µm sample looks like a 2

$\times$ 2 array of 2D PhCs, and in the following we will consider one of these samples, displaying optimal matching between peak absorption and photonic modes.

3. Optical measurements

Experiments of reflection modulation were performed in a pump-probe set-up with laser sources delivering 130 fs optical pulses at a repetition rate of 80MHz. The output from a Ti:Sa laser at 810 nm supplies the pump pulses, while the probe is provided by the output beam of an optical parametric oscillator, tunable around 1.55 µm. The samples are explored in the surface normal configuration, with both pump and probe focusing on to the sample via a 10X microscope objective to spot sizes of $\approx$40 µm and 15 µm respectively. The temporal delay between pump and probe is controlled by varying the probe optical path. Reflected signal is collected through the same objective and detected by a fiber-coupled optical spectrum analyzer (OSA).
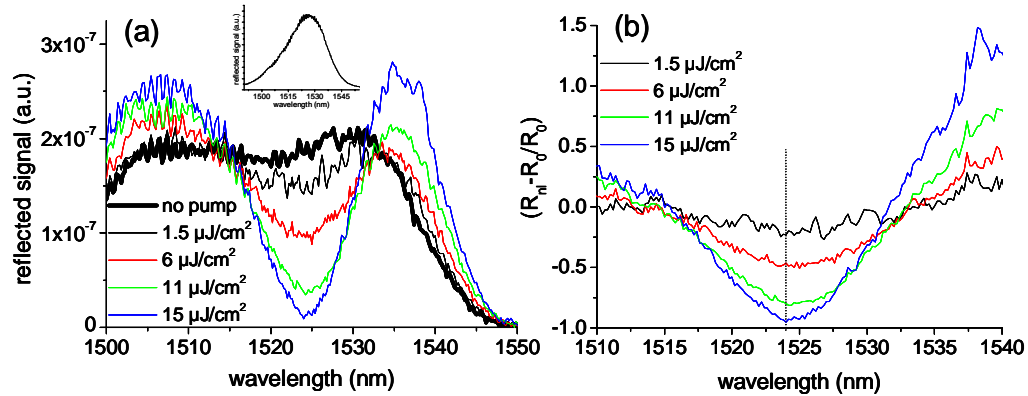

Fig. 2. (a). reflected probe signals (not normalized) versus pump fluence at 810nm. The bold black curve corresponds to the case where the pump is off. The inset shows the reflected spectrum from a reference gold mirror. (b) Differential reflectivity for different values of pump fluence. The dotted line at 1524 nm indicates where contrast ratio is maximum. Both (a) and (b) refers to the same sample zone, labeled as C.

Figure 2(a) represents the reflected spectra from one of the four zones of the sample for different pump levels. The central wavelength of the input probe beam is at $\approx$1526 nm. The spectral shape of non-normalized reflected pulses is here strongly distorted because of the resonant PhC mode and absorption. Figure 2(b) shows the differential reflectivity $(R_{nl}-R_0)/R_0 \equiv \Delta R/R_0$, where R_{nl} is the power-dependent reflectivity value, and R_0 the pump-off reflectivity [bold spectrum in Fig. 2(a)]. Looking at the spectra in Fig. 2(a), we remark that the identification of the photonic band is easier when the pump is on, whereas in the pump-off reflection spectrum the dip is very broad. As the incident pump level grows, an increasingly deep minimum appears due to absorption saturation. Note that the temporal delay between the pump and probe pulses is chosen to get the highest reflection modulation at the resonance wavelength, which is 1524 nm. This corresponds to the maximum photo-carrier density created by the pump, before recombination processes take over.
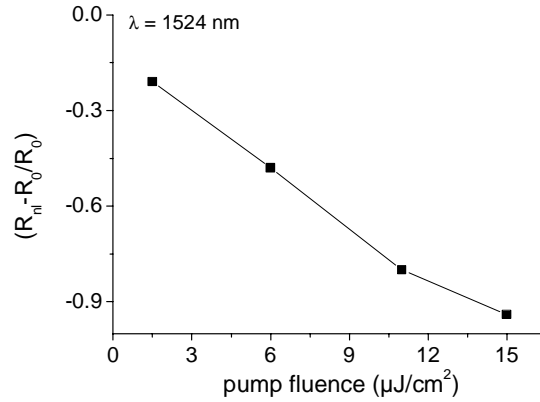
Fig. 3. Differential reflectivity measured from zone C at 1524 nm, as a function of pump fluence.

In Fig. 3, we plot the differential reflectivity measured at the center of the photonic resonance as a function of external pump fluence. The modulation of the reflectivity is as high as 94% when the pump fluence is 15 $\mu J/cm^2$. Note that, in this experiment, thermal effects appear to be negligible. Indeed, no relevant red shift of the photonic mode was observed. The excitation regime (a 130fs pulse every 12ns) and the presence of the bonded substrate are the reasons for this behavior. Of course, if the repetition rate of the excitation was increased, thermal effects could induce a spectral red-shift of the operation wavelength.

The dynamic response of the differential reflectivity is shown in Fig. 4 for a pump fluence of 11 $\mu J/cm^2$. Zero time delay is set at the maximum (absolute) change of reflectivity. The sharp drop for negative delay is related to capture time into the wells. The measured value of 13 ps (rise time) is consistent with results reported in literature [22]. On the other hand, the time the reflectivity takes to recover to its initial value is of course the carrier recombination time. The exponential fit gives a time decay around 215 ps. This value is shortened as compared to typical decay time measured for the unpatterned quantum well system, around 700 ps, due to enhanced recombination at the hole walls [8].
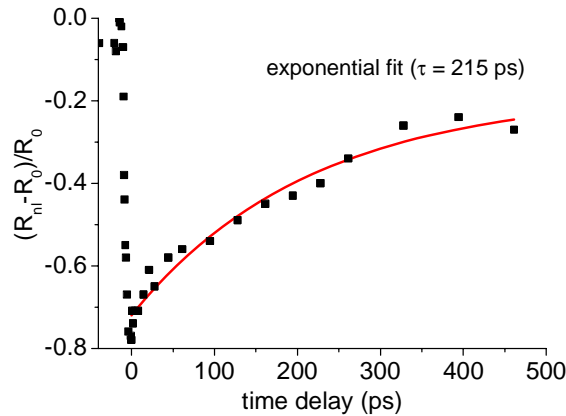

Fig. 4. Dynamic response of the reflectivity for pump fluence of 11 $\mu J/cm^2$. The origin of the time axis is set at the maximum change of reflectivity.

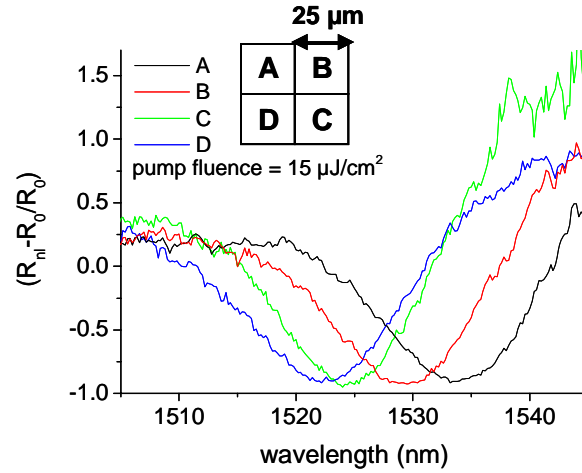We observed similar behavior in reflection from zones A, B, and D.

Fig. 5. Differential reflectivity from the four samples in the case of pump fluence equal to 15 µJ/cm². The inset shows the 25 µm x 25 µm A, B, C, D adjacent zones of the sample.

Figure 5 shows the spectral shift of the dip in differential reflectivity obtained when the beams are moved across adjacent samples. A variation of ≈5 nm in the air-hole radius between samples A-B, B-C and C-D produces a spectral shift (measured between minima) of around 4 nm. The reflectivity modulation achievable in the four samples for the same pump levels is comparable. Outside the resonance, carrier-induced effects vanish. The change in reflectivity is greater than 80% over a 5 nm bandwidth for each zone, giving a total bandwidth for the system of (4x) 5 nm. In principle, this total bandwidth could be extended to (Nx) 5 nm by defining N zones of different lattice parameters. This would be useful for the design of future broad-band applications.

4. Discussion and conclusion

In Table 1, we compare the relevant parameters of this system to other results previously reported in literature.

Table 1. Comparison among several optical studies of 2D PhC structures. The row in bold corresponds to the present work.

material	layout	λ (nm)	µJ/cm²	τ (ps)	$\Delta R/R$	$\Delta\lambda$ (nm)	ref.
Si	S	1900	1300	>1000	60%	30	[5]
InP/InAsP QWs on Silicon	S	1520	65	90	67%	0,5	[6]
InP/InGaAs QWs on Silicon	**S**	**1530**	**15**	**215**	**94%**	**(4x) 5**	
InAs QDs on GaAs	G	1300	66(*)	60	68%	10	[7]
AlGaAs/GaAs QWs on GaAs	S	1490	300	13	96%	5	[8]
AlGaAs/InAlGaAs QWs on GaAs	S	830	1300	9	66%	5	[9]

(*) pump fluence coupled into the waveguide

Different active PhC systems are presented. For every system, we indicate the material used, geometrical layout (S for surface configuration, G for guided configuration), operation wavelength, pump fluence, carrier recombination time, differential reflectivity and the bandwidth deduced from the quoted references. The systems considered here are based on

either Silicon, InP or GaAs materials. From the table, we see that GaAs-based systems are better for ultrashort response times enabling high speed modulation. This point is inherent in the choice of semiconductor material. The other aspect that comes out clearly is related to the design of the PhC structure, which is an important factor in order to obtain modulation contrast of the order of 90%. Our system gives a good tradeoff for fast operation, high contrast and low-pump fluence.

In conclusion, we have fabricated 2D InP/InGaAs PhCs on top of a Silicon wafer by means of BCB bonding technique, a promising technology as it enables the integration of emitting and nonlinear devices onto a silicon-based photonic circuit. We have demonstrated that these structures may be used as fast optical modulators operating at telecom wavelength where 90% change in reflectivity is obtained by saturating the absorption of the QWs embedded in the PhC slab. The nonlinear regime of interest is reached with a pump fluence of the order of 10 µJ/cm^2. As compared to conventional semiconductor microcavity modulators, our system is simpler to grow but more demanding from the processing point of view. Still, the photonic band engineering makes the 2D PhCs better suited for broad bandwidth application as the operating wavelength can be tuned spatially. Finally, the inherent 2D planar technology and the good coupling efficiency between free-space and resonant Bloch modes is promising for monolithic 2D arrays of PhCs for all-optical data processing.

Acknowledgment